

ABSTRACT

KELLEY, RICHARD LEE. Plant Virus Nanoparticles as Targeting Agents: New Tools for Cell Biology. (Under the direction of Stefan Franzen.)

In order to develop *Red clover necrotic mosaic virus* as a novel drug carrier to target specific cancer cells, the structure and viability of a prospective plant viral nanoparticle was studied. Initially, the assembly process of the virus was duplicated *in vitro* using transcript RNAs and capsid protein harvested from disassembled wild type virus. Using virus obtained by the preferred method of plant propagation, wild type virus was evaluated *in vivo* and gave no deleterious effects. The mice suffered no acute toxicity, no detected immune response and no evidence of biodistribution in any internal organs. With an understanding of preliminary toxicity, a formulation to target HeLa cells was produced to verify and expand on *in vitro* and *in vivo* testing results. The initial attempt at cell targeting visualization using a luciferin/luciferase luminescence indicator did not provide conclusive evidence of cellular uptake.

Plant Virus Nanoparticles as Targeting Agents:
New Tools for Cell Biology

by
Richard Lee Kelley

A thesis submitted to the Graduate Faculty of
North Carolina State University
in partial fulfillment of the
requirements for the degree of
Master of Science

Chemistry

Raleigh, North Carolina

March 13, 2009

APPROVED BY:

Dr. Steven A. Lommel

Dr. Tatyana I. Smirnova

Dr. A. Clay Clark

Dr. Stefan Franzen
Chair of Advisory Committee

DEDICATION

This work is dedicated to, first and foremost, my partner in life, Charles Ernest Leathers, Jr., my mother, Lois Jean Burkepile, my father and stepmother, Michel Lee and Katrina Kelley, and my dear friends, Diana Kay Kelley, Jack Leland Dovey, and Patricia Jean Dovey.

BIOGRAPHY

Richard Lee Kelley was born on June 6, 1967 into the family of Michel Lee and Lois Jean Kelley. After graduating from Spencer High School in Spencer, West Virginia, Rich began his undergraduate studies with a double major in Chemistry and Biology at Marietta College, in Marietta, OH in the fall of 1985. After an extended hiatus from undergraduate studies, Rich resumed his education with a double major in Chemistry and AYA, Integrated Science Education at Ashland University in Ashland, OH in the fall of 2000. While at Ashland University, Rich conducted research in the laboratory of Dr. Perry Corbin attempting to develop a silver-containing polylactide polymer for use as a hydrogel in the treatment of burn victims. In the Spring of 2004, Rich received a Bachelor of Science in Chemistry and a Bachelor of Science in Education, AYA Integrated Science, with a minor in Physics. In the fall of 2005, Rich entered the graduate program at North Carolina State University in Raleigh, NC. He began graduate research under the advisement of Dr. Stefan Franzen in the spring of 2006. His research focused on the development of a plant virus, *Red clover necrotic mosaic virus (RCNMV)* as a nanoparticle for the treatment of disease. His research focused on new ways to propagate the plant virus, and *in vitro* and *in vivo* assessment of the viability and efficacy of RCNMV as a nanoparticle.

ACKNOWLEDGEMENTS

First, I would like to thank my partner, Charles E. Leathers, for his unending love and source of strength. I would especially like to thank my family and friends for their unwavering support and encouragement. Including, my father and stepmother, Michel Lee and Katrina Kelley, my mother, Lois Jean Burkepile, my brother and his family, Robert Michel Kelley, Benjamin Harrison, Joshua Robert, Timothy Michel, Laura Beth, my baby brother and his family, Jeremy Clark, Sheryl Lynn, Sara Marie, Samantha Nicole, Sabrina Paige, Sydney Rose, my ex-sister-in-law, Sonia Sue Kelley, my stepbrother and sister-in-law, Scott and Penny Miller, my stepsister and her family, Tammy, Cassandra and Kelley, my youngest stepsister Heather, and her daughter, Savannah. Also, I would like to acknowledge my dearest friends, Diana Kelley, Jack Dovey, Patricia Dovey, John Rowsey and Janice Rowsey.

I would like to acknowledge the undergraduate faculty at Ashland University, particularly my undergraduate research advisor, Dr. Perry Corbin.

I would especially like to thank and acknowledge the Chemistry department staff and faculty at North Carolina State University and my graduate research advisor, Dr. Stefan Franzen, for the opportunities in research and teaching I wouldn't have had otherwise. Additionally, I would like to acknowledge Dr. Steve Lommel and his research group in the Virology department at NC State. Also, I would like to acknowledge the other two members of my committee, Dr. A. Clay Clark and Dr. Tatyana Smirnova. Finally, a special thanks to all of the people in the Franzen group I've had the fortune to work beside over the last several years. Your support and collaboration has been greatly appreciated.

TABLE OF CONTENTS

LIST OF TABLES.....	vii
LIST OF FIGURES.....	viii
1. An Introduction to Plant Viral Nanoparticles	
1.1 An Introduction to Plant Viral Nanoparticles.....	1
1.2 <i>Red clover necrotic mosaic virus</i>	3
1.3 Development of a Plant Viral Nanoparticle.....	4
2. Theory of Plant Viral Nanoparticle Development and Testing	
2.1 Alternative Propagation Methods for RCNMV.....	6
2.2 In Vivo Testing of RCNMV.....	6
2.3 Development of a PVN to Verify Cellular Uptake.....	7
3. In Vitro Assembly of a Plant Viral Nanoparticle	
3.1 Introduction.....	8
3.2 Assembly of plant viral nanoparticles using transcript RNA's and coat protein harvested from wild type RCNMV.....	9
3.3 Transcript production.....	10
3.4 Coat protein purification.....	12
3.5 In vitro assembly of virus-like particles.....	17
3.6 Encapsidation of the CBDwt-MBP/ISO-s protein by a plant viral nanoparticle.....	21
4. <i>In vivo</i> testing of RCNMV in Nude mice	
4.1 Introduction.....	25
4.2 Preliminary assessment of Acute Toxicity and Preliminary Bioaccumulation in Nude mice.....	25
4.3 Virus Production.....	26
4.4 Delivery of RCNMV to Nude Mice.....	26
4.5 Results and Discussion.....	28
5. Acute Toxicity, Immunogenicity, Clearance and Preliminary Biodistribution <i>in vivo</i>	
5.1 Introduction.....	30
5.2 PVN Dose limit.....	30
5.3 Immunogenicity of PVN.....	31
5.4 Radiolabeling of PVN.....	31
5.5 Clearance rate determination and preliminary biodistribution.....	32
5.6 Results and Discussion.....	33

6.	In Vitro Luminescence of Luciferin-infused RCNMV Conjugated with Adenoviral Derived Targeting Peptides.	
6.1	Introduction.....	40
6.2	Infusion of Luciferin into RCNMV [5].....	40
6.3	Conjugation of Targeting Peptides [32,33].....	41
6.4	Preparation of samples and delivery to HeLa-luc luciferase expressing cells.....	42
6.5	Results and Discussion.....	44
7.	Conclusion.....	47
	References.....	49

LIST OF TABLES

Table 1. UV-VIS absorbance of pooled mouse plasma samples as determined by ELISA.....	35
Table 2. Average counts of random urine samples at varied time points.....	39
Table 3. Sample identification for delivery to HeLa-luc cell plates.....	42

LIST OF FIGURES

Figure 1: Infusion of therapeutics and targeting peptide conjugation of a spherical plant virus.....	2
Figure 2: Cryo-electron Microscopic images of RCNMV [5].....	4
Figure 3: RCNMV transcript reassembly scheme.....	9
Figure 4: In vitro assembly schemes for proposed PVNs	10
Figure 5: Transcripts of linearized plasmids.....	12
Figure 6: 12% SDS/Page gel of RCNMV disassemblies from pH2-pH10....	14
Figure 7: SDS/Page gel of purified coat protein.....	15
Figure 8: Centricon 100,000 MWCO centrifugation filter.....	15
Figure 9: Interaction of RNA-1 with the stem loop secondary structure of RNA-2 to form nucleation site for encapsidation.....	17
Figure 10: Assembly scheme for wtRCNMV particles.....	18
Figure 11: Virus-Like Particles, 300,000x magnification	20
Figure 12: Dynamic Light Scattering for Size of Virus-Like Particle.....	20
Figure 13: Agarose gel electrophoresis of DNA-2 conjugated CBDwt-MBP/ISO-s Protein.....	23
Figure 14: TEM images of CBD PVN – Trial 1.....	24
Figure 15: Whole Body fluorescence images of Nude mice.....	27
Figure 16: Fluorescence of RCNMV-FITC suspensions at t=1 hour.....	29
Figure 17: Circulating ¹³¹ I-labeled RCNMV as determined by detectable radioactivity in mouse plasma.....	36
Figure 18: Standard curve of luciferin dosed to HeLa-luc cells.....	44
Figure 19: Luciferin only controls at 30min time point for HeLa-luc plates...	45

Chapter 1

Introduction

1.1 An Introduction to Plant Viral Nanoparticles.

Red clover necrotic mosaic virus (RCNMV) presents an excellent prospect as a platform for the development of a nanoparticle for varied uses from the research laboratory to the pharmaceutical industry. In an article in the May 14, 1998 issue of *Nature*, researchers at Temple University explored the uses of plant viruses for the development of materials sciences, drug delivery systems, etc. They noted that plant viruses “are incredibly host-specific”, consumed by humans in vegetation, which is part of a regular daily diet, and can “have their genetic material removed, leaving only a coat which can be used as a container” [1]. Even without removal of the native genome, it is possible to attenuate the virus to eliminate or limit infectivity within native plant species. These benefits highlight the advantages of using a plant virus as a nanoparticle. Plant viruses are more versatile in cell biology applications than alternatives such as liposomes, polymers and solid nanoparticles. For instance, liposomes are not as structurally sound and have distinct disadvantages such as nuclear localization capability. Plant viral nanoparticles have the potential to revolutionize the way we analyze cellular processes, treat disease, and conduct gene therapy. With their already extensive exposure in animal hosts and relatively simple structures, plant viral nanoparticles (PVN) provide new avenues for the development of

intracellular assays. Such assays can have impact on studies of cell signaling, understanding the cell cycle or modulating gene expression. The applications of PVNs can also extend to novel drug delivery systems.

The spherical capsid and internal cage structure of some plant viruses have proven to be effective for the encapsulation of materials or infusion of small molecules[2,3] with conjugation of targeting peptides[4,5] (Figure 1) that can be used for targeted delivery of fluorescent sensors and therapeutics. To understand the unique challenges in altering the function and production of plant viruses as a drug delivery system, it is necessary to understand the basic

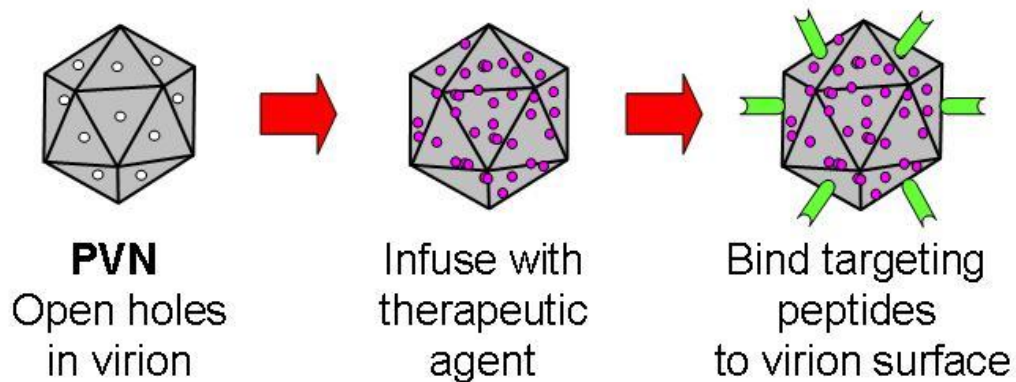


Figure 1: Infusion of therapeutics and targeting peptide conjugation of a spherical plant virus.

properties and structure of viruses. Viruses are cellular parasites that hijack the replication machinery of the host cell and suspend most endogenous cellular activity. Their structure consists of nucleic acid, either DNA or RNA, which is surrounded by a protein shell that may or may not contain a lipid envelope. Viral genomes can be non-segmented, consisting of a single nucleic acid molecule, or

segmented, consisting of more than one nucleic acid molecule. The nucleic acid molecules of a virus can be contained within a single virus or separated into multiple viruses. Viruses do not express their own ribosomal RNA. Therefore, they must subvert the machinery of the host cell, which suspends cellular activity resulting in cell death. Viruses contain structural and non-structural proteins (not present in the dormant particle). Viruses are small parasitic particles which are spherical, helical or bacilliform in shape.

1.2 *Red clover necrotic mosaic virus*

RCNMV is a member of the genus *Dianthovirus* in the family *Tombusviridae*. These viruses are non-enveloped with an icosohedral sphere of approximately 32-35nm in size. RCNMV contains a positive sense, single stranded bipartite genome. There are 2 RNA segments of 3,890bp and 1,448bp, which interact to form the origin of assembly for capsid protein (CP) nucleation and ultimately encapsidation of the nucleic acid. It has been reported that a second assembly scheme exists in which multiple copies of RNA-2 form the origin of assembly and are encapsidated [6]. RNA-1 contains an open reading frame that codes for a 36kDa coat protein and –1bp frameshift reading frame which codes for an 88kDa RNA-dependent RNA polymerase[7]. RNA-2 codes for a 35kDa movement protein. The capsid consists of 180 copies of the capsid protein, which exists in 3 different conformations and orient to form 3 different domains (Inner, Shell, and Protruding) within the capsid (Figure 2a). The inner

domain interacts with the viral RNA to form a cage structure (Figure 2b) with a 17Å diameter [8].

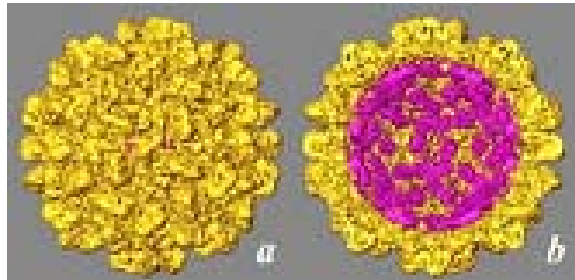


Figure 2: Cryo-electron Microscopic images of RCNMV [5]

The protruding domain contains 2 surface Lysines and a Cysteine where 4-(N-Maleimidomethyl)cyclohexanecarboxylic acid N-hydroxysuccinimide (SMCC) linking chemistry can be used to attach peptides or other cell-targeting molecules. The outer domain permits the multivalent presentation of ligands,[9,10] which can give unique functionality to the virus in the form of surface receptor recognition for cell targeting. Additionally, the surface can be PEGylated to alter the chemical properties of RCNMV to change the rate of uptake or systemic retention. However, conjugating peptides to the virus surface may not be ideal in certain applications.

1.3 Development of a Plant Viral Nanoparticle

Efforts are under way to use plant viruses as nanoparticles for the development of materials science, drug delivery systems, etc. [20] Plant viruses

are more versatile in cell biology applications than alternatives such as liposomes, polymers and solid nanoparticles. Plant viral nanoparticles (PVN) promise to revolutionize the way we analyze cellular processes, treat disease, and conduct gene therapy. With their already considerable exposure in animal hosts and relatively simple structures, plant viral nanoparticles (PVN) provide new avenues for the development of intracellular assays. Such assays can have impact on studies of cell signaling, understanding the cell cycle or modulating gene expression. The applications of PVNs can also extend to novel drug delivery systems. The spherical capsid and internal cage structure of some plant viruses have proven to be effective for the encapsulation of materials or infusion of small molecules[21,22] with conjugation of targeting peptides[23,24] to the PVNs surface which can be used for targeted delivery of fluorescent sensors and therapeutics. The structure of, *Red clover necrotic mosaic virus* (RCNMV), is ideal for exploration as a drug delivery system.

Chapter 2

Theory of Plant Viral Nanoparticle Development and Testing

2.1 Alternative Propagation Methods for RCNMV

Currently, viral progeny are produced from *in vivo* propagation of the virus in *Nicotiana clevelandii*, a type of tobacco plant. This is primarily done by two methods: (1) infecting with transcripts produced *in vitro* from cDNA clones of the viral RNAs inserted into an expression plasmid in which the T7 polymerase promoter and terminator have been cloned[11] and (2) harvesting viruses from plants which have been through several infection cycles. It is worthwhile to explore optional methods in the propagation of virus and production of PVNs, which will eliminate the need for greenhouse space, reduce the amount of time required to produce nanoparticles, and control cross-contamination of experimental plant populations and indigenous species by genetically altered viruses. These include heterologous gene expression organisms such as *Escherichia coli* (*E. coli*), *Saccharomyces cerevisiae* (Bakers Yeast), and *Pseudomonas fluorescens* (*P. fluorescens*). It has previously been shown that virus-like particles can self-assemble in these expression systems[12-14].

2.2 In Vivo Testing of RCNMV

An area of concern in any prospective viral delivery system is the potential for harm to the human host. A preliminary *in vivo* animal study was conducted to gauge the feasibility of more extensive animal testing on final

formulations of the proposed delivery vector. This study was a launching point to explore *in vivo* toxicity testing, antigenicity and tumor targeting in animal models. With a better understanding of the effect of the PVN *in vivo*, it is worthwhile to develop potential applications.

2.3 Development of a PVN to Verify Cellular Uptake

RCNMV provides an ideal platform to develop a multifunctional particle with specific functionalities in biomedical applications. It is now possible to develop a biological tool to be implemented towards the improvement of a wide variety of therapeutic treatments, such as enhanced MRI imaging, understanding cellular signaling pathways, visualizing cellular function, and localized treatment of disease. Virus-like particles provide a stable environment as a vehicle for pharmaceuticals, imaging agents, or other small molecules. With a cargo securely packaged and with the addition of the appropriate targeting peptide, the PVN can now be delivered to a specific cell type. With this in mind, it is necessary to develop novel methods of packaging a variety of types of materials and giving function to form. It has been previously shown that an Adenoviral-derived targeting peptide when linked to a gold nanoparticle will internalize to the nucleus of a cell[33]. In addition, an RCNMV molecule can be infused with a cargo, doxorubicin, and delivered to HeLa cells using another Adenoviral targeting peptide, CD46. An attempt was made to verify these results using a luciferase-expressing HeLa cells with Luciferin as the infused cargo.

Chapter 3

In Vitro Assembly of a Plant Viral Nanoparticle

3.1 Introduction

In vitro assembly is a controlled method to propagate engineered virus-like particles (VLPs). With *in vivo* propagation, there is a possibility of introducing contaminants into the sample during the process of purifying virus particles from plant homogenate. In addition, propagation of virus from plants has other disadvantages, such as the need for a significant amounts of greenhouse space and the time involved in maintaining plants, inoculating plants with virus, harvesting, etc. A controlled laboratory setting with minimal use of space would be preferable. To accomplish *in vitro* assembly, transcripts of viral RNA genes cloned into PUC expression vectors and transformed in a DH5 α strain of *E. Coli* were produced either comparable to those of the wild type RCNMV, or cloned to provide an altered functionality. The transcripts were characterized using UV/VIS spectroscopy and agarose gel electrophoresis and verified against plasmid DNA. Additionally, coat proteins were isolated and purified from disassembled wild type RCNMV and their presence was confirmed by UV/VIS and SDS/Page gel electrophoresis. Virus-like particles were made by dialyzing the components against a buffer optimized for viral assembly (Figure 3).

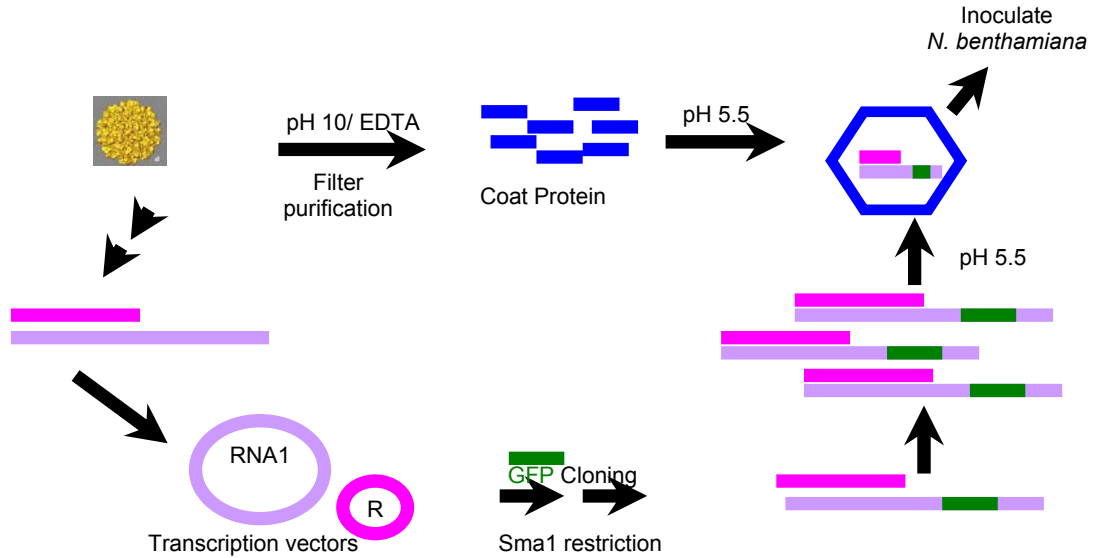


Figure 3: RCNMV transcript reassembly scheme

Dynamic Light Scattering (DLS) and Transmission Electron Microscopy imaging (TEM) were carried out to confirm success.

3.2 Assembly of plant viral nanoparticles using transcript RNA's and coat protein harvested from wild type RCNMV

To understand the ability of RCNMV virus-like particles to self-assemble and be viable, 3 experiments (Figure 4a, 4b, 4c) were designed to mimic known wild type RCNMV assemblies and observed phenomenon *in vivo*. Experiment 1 (Figure 4a) and 2 (Figure 4b) were designed to mimic wild type viruses. In Experiment 3 (Figure 4c), an RNA-1 clone has been produced where the coat protein gene has been replaced with the gene for green fluorescing protein (GFP). As an additional experiment (Figure 4d) in functional encapsidation, an

assembly reaction (Figure 4d) was attempted with a protein developed in the Hahn group at The University of North Carolina.

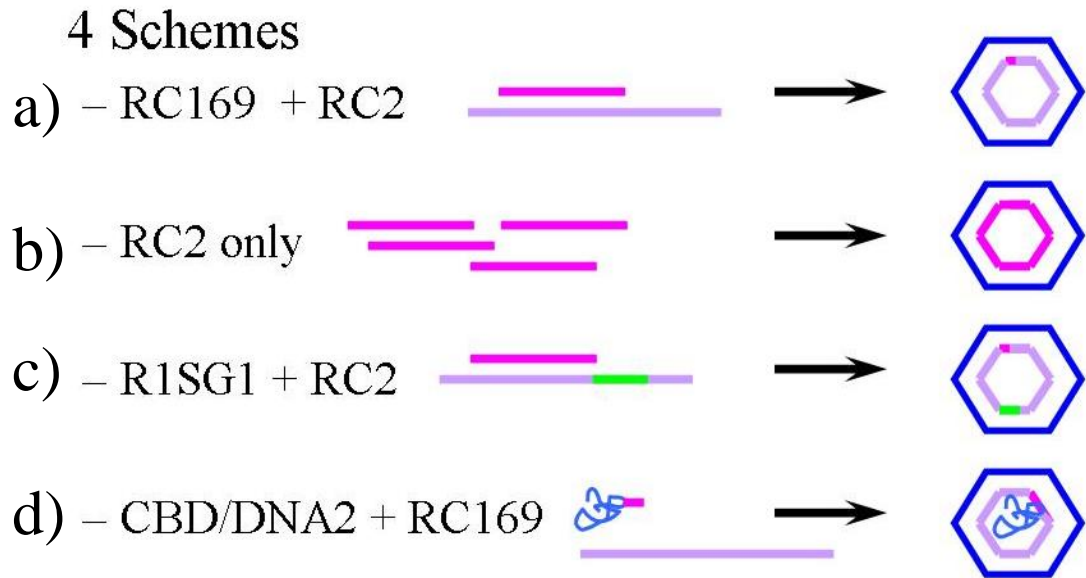


Figure 4: In vitro assembly schemes for proposed PVNs: (a) wtRCNMV particle containing transcripts of RNA-1 and RNA-2 (b) wtRCNMV particle containing transcripts of RNA-2 only (c) particle containing RNA-1 transcript that has the gene for green fluorescing protein in place of coat protein gene and (d) CBD fret signaling protein conjugated to DNA2 with RNA-1 transcript.

3.3 Transcript production

Viral transcripts of the segmented genome of RCNMV were made by cloning cDNA strands of each respective RCNMV ssRNA into empty expression vectors containing the T7 polymerase promoter and terminator. These plasmids were provided by the Lommel Research Group in the Plant Pathology department at North Carolina State University. Plasmid samples were transformed in a DH5 α strain of *E. coli* and purified using a QIAprep Spin

Miniprep DNA Purification Kit (QIAGEN Catalog # 27104). The Circular plasmids were then linearized using SmaI restriction enzyme (Fisher Scientific Catalog # PR-R6121) complementary to a SmaI restriction site cloned into the plasmid upstream of the T7 Promotor. Transcription reactions were completed on the linearized plasmids using an Ambion MEGAscript® T7 High Yield Transcription Kit (Catalog # AM1333). Each reaction vial was treated with RQ1 RNase-Free DNase (Promega Catalog # M6101) as directed to digest the double stranded plasmid DNA. A phenol:chloroform extraction was done on each sample and the aqueous phase retained for extraction of the RNA transcripts. Ethanol precipitation of the RNA in 90% ethanol/water was followed by a 70% ethanol wash to remove excess nucleotides and miscellaneous detritus. Excess ethanol was removed by evaporating with a Savant AES-1000 Automatic Environmental Speedvac. The transcript RNA was then resuspended in 50µL nuclease-free water provided in the Ambion transcription kit.

After optimization of the transcription reaction, significant concentrations of RNA transcripts were produced and analyzed via Agarose gel electrophoresis (Figure 5) and UV/VIS spectroscopy. The transcripts and wild type RNA molecular weights were compared against a DNA molecular weight marker to verify the size and similarity of the RNA's. UV/VIS spectroscopy was used to verify the presence (absorbance at 260nm) of RNA and calculate the concentration for each sample.

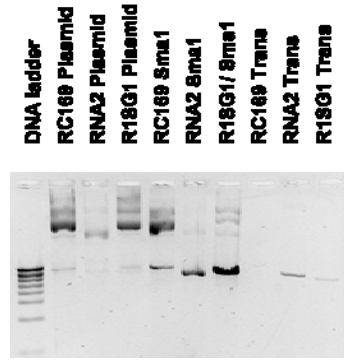


Figure 5: Transcripts of linearized plasmids.

3.4 Coat protein purification

Coat protein was harvested from wild type virion after disruption of the viral capsid by the addition of 50mM EDTA at high pH, ~10. RNAs were removed from disassembly mixture by lithium chloride precipitation. The supernatant was removed using a 100,000 molecular weight cut-off (MWCO) Centricon centrifugation filter. To confirm the presence of protein, the filtrate was analyzed by SDS/Page gel electrophoresis and UV/VIS absorbance. When compared to a protein marker, there were no bands corresponding to the correct size for the coat protein in the 12% SDS/Page gel. A UV/VIS profile of the sample indicated a small, broad peak in the appropriate location, $\lambda_{\max} \sim 280\text{nm}$, for a protein. To verify the disassembly process, 500 μL of wild type RCNMV, 5mg/mL, was placed in a 10,000 MWCO Pierce Slide-A-Lyzer Dialysis Cassette (Pierce, Cat #66383) and stirred overnight in disassembly buffer at pH10. Empirical observation has shown the coat protein to be insoluble at pH's 5-9

After approximately 8-10hr, the presence of a white, clumpy aggregate, indicated the presence of coat protein after disassembly of virus. A critical concentration of coagulation was determined for viral disassembly by decreasing the concentration of wtRCNMV and following the previous protocol. At 1mg/mL of RCNMV, the coat protein aggregates were no longer seen in the dialysis cassette. It was hypothesized that initial attempts to identify coat protein failed due to insolubility of the protein at mid-range pH's in 50mM EDTA buffer, up to and including pH10.

Previous VLP assembly reactions were carried out at pH 5.5 [2]. RCNMV were disassembled within a pH range from 4 to 10 to determine relative coat protein solubility, which was chosen to span previous assembly and disassembly reactions. Inconclusive results prompted expansion of the pH range of pH 2-12. After purification with a Centricon YM-100 100,000 molecular weight cut-off centrifugation filter, SDS-PAGE gel electrophoresis showed coat protein bands (Figure 6) at pH 2 and pH 11, at the appropriate 36kDa level. At these pH extremes it is likely that the coat proteins have been completely or partially denatured.

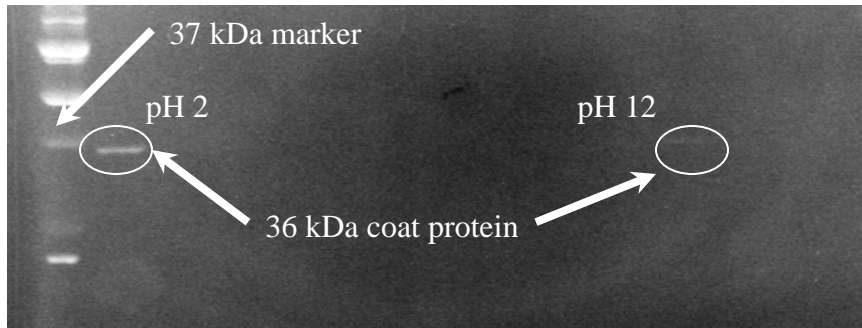


Figure 6: 12% SDS/PAGE gel of RCNMV disassemblies from pH2-pH10.

Thus, refolding events may not occur and the coat protein would not be able to correctly interact to form the capsid. Assembly reactions were attempted with these protein samples and no formation of VLPs could be confirmed. In an attempt to increase the solubility of the coat protein, various salts of 10mM concentration were added to the disassembly buffer including: sodium acetate (NaOAc), NaCl, KCl, and Tris. No appreciable increase in solubility could be identified by SDS/PAGE gel electrophoresis. Although, significant increases in UV/VIS absorbance were seen when adding Tris or NaOAc. Therefore, the concentration of EDTA was increased to 100mM and the concentration of TRIS was increased to 20mM. However, this method does not provide a significant amount of coat protein. When run through a Centricon (Figure 8), the filtrate contained a minimal amount of coat protein as indicated by the faint band (Figure 7b) in an SDS/PAGE gel. By contrast, the retentate contained a significant amount of protein (Figure 7c).

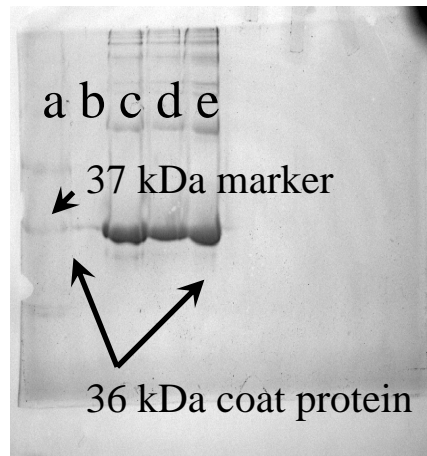


Figure 7: SDS/PAGE gel of purified coat protein. (a) Protein marker (b) Centricon filtrate (c) retentate (d) disassembled RCNMV (e) wtRCNMV.

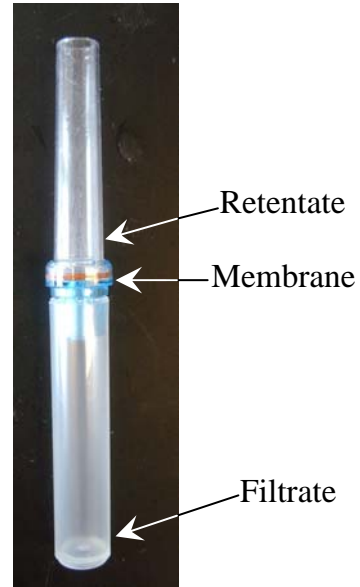


Figure 8: Centricon 100,000 MWCO centrifugation filter.

Dynamic Light Scattering (DLS) of the disassembled RCNMV confirmed no particles of significant size within the desired 32-35nm range. Therefore, it was concluded that the coat proteins were either aggregating as they were concentrated at the membrane or that they were sticking to the membrane of the Centricon. Additional methods of protein purification were attempted on the coat protein of disassembled RCNMV, including: Gel Permeation Chromatography (GPC), Ion Exchange Chromatography (IEX), and Hydrophobic Interaction Chromatography (HIC). For GPC, three different gels (BioRad BioGel A-0.5m, exclusion limit of 500,000 daltons, GE Healthcare Sephacryl S-300, exclusion limit of 1,000,000 daltons, Sigma Sephadex G-75, exclusion limit of 500,000

daltons) were attempted that matched the pH range of the disassembly buffers and size of the coat protein. Each column was packed per manufacturer's instruction and equilibrated with buffer prior to use. The column was validated for packing efficiency with a 1% acetone solution. Blue Dextran (MW 2,000,000) was run through the column to determine the void volume of the column and a molecular weight profile was acquired using BioRad Gel Filtration Standards (Catalog #151-1901). Disassembled RCNMV samples were added to each column at a rate of 60 drops per minute, 2mL fractions collected, samples stained with Coomassie Blue Indicator and analyzed for UV/VIS absorbance (490nm) in a BioTek Synergy HT plate reader. Successful determination of the molecular weight profile and elution of Blue Dextran confirmed the activity of the columns, but no indication of RCNMV purified coat protein was seen in any of the collected fractions. Additionally, buffers with varied ionic strength and pH were used with no increase in protein solubility. The same results were obtained using Anion Exchange Chromatography (BioRad Macro-Prep High Q Strong Anion Exchange Support) and Affinity Chromatography (Sigma *p*-aminobenzyl-1- β -glactopyranoside agarose). Also, alternative centrifugation devices (Nalgene-Nunc, Catalog #191-2080, 0.8 μ m syringe filter; Whatman Anotop 25, Catalog #6809-2022, 0.2 μ m Syringe filter; Amicon Microcon 100, Catalog #42413, 100,000MWCO) were used that resulted in no significant increase in concentration of coat protein over what was achieved using the Centricon. It is

This forms the origin of assembly for nucleation of the capsid proteins to begin encapsidation of the nucleic acid. Additionally, RNA-2 can interact with a homologous sequence on another RNA-2 to form an origin of assembly (Figure 10). VLP's were assembled by incubating RNA

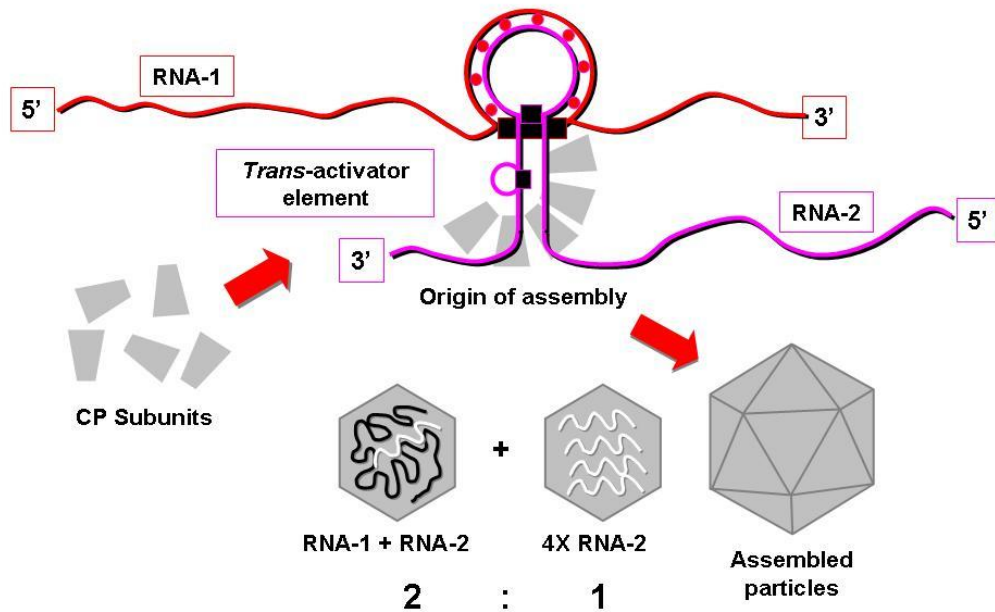


Figure 10: Assembly scheme for wtRCNMV particles.

transcripts in a microcentrifuge tube for ~15 minutes, then adding coat protein in a 200:1 coat protein:transcript mole ratio. Contents of tubes were placed in uniquely identified Pierce Slide-a-lyzer dialysis cassettes and dialyzed against a 100mM Tris Buffer, pH5.5 [2]. 20mM sodium acetate was added to buffer based on increase in coat protein stability reported earlier. After stirring overnight, cassettes were removed from buffer baths and 20mM each of calcium chloride and magnesium chloride was added to aid in stabilization of the nanoparticles.

The cassettes were returned to their respective buffer baths and stirred for an additional 4 hours. After the final incubation period, the contents of the dialysis cassettes were removed and placed in microcentrifuge tubes for future analysis. Transmission Electron Microscopy (TEM) was used to image the particles and DLS were used to analyze the distribution of particle sizes. TEM images at 300,000x magnification were taken confirming the presence of each particle (Figure 11a, 11b, 11c). When compared to the reference bar, the particles seem to be of a uniform size of ~28nm. In addition, they exhibit the icosohedral symmetry typical of the *Dianthoviruses*. Dynamic Light Scattering confirms the findings from TEM imaging. Particle size for the RC169/RC2, RC2 only, RC1SG1/RC2 VLP's are 28, 29, and 31nm respectively. The particles sizes are slightly smaller than the size of 32-35nm reported previously for RCNMV [2].

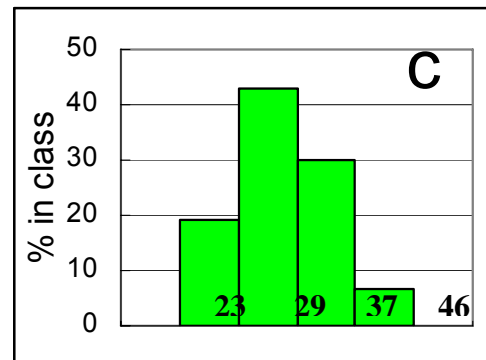
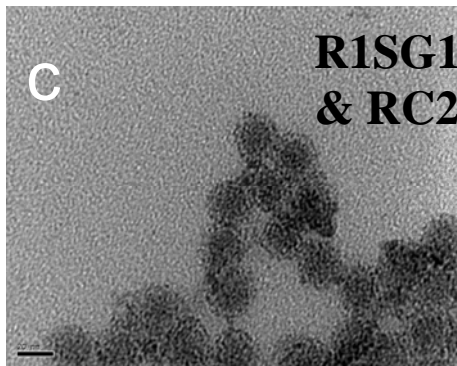
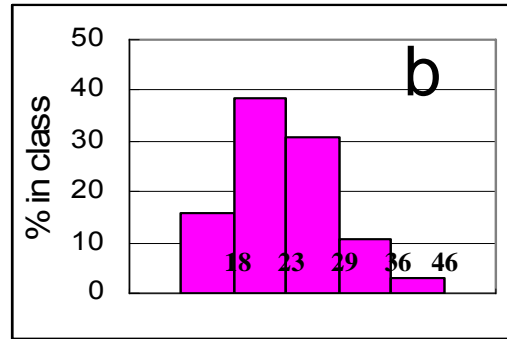
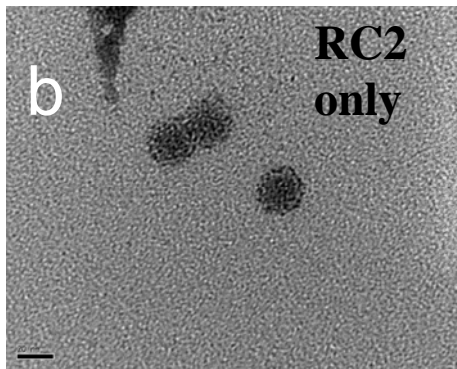
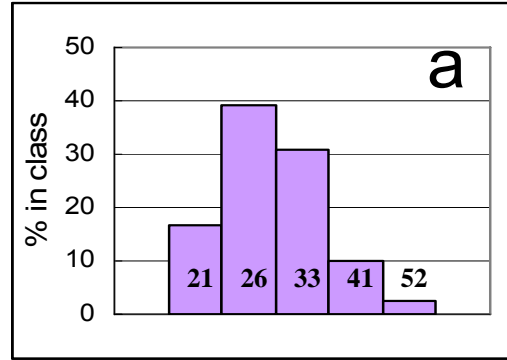
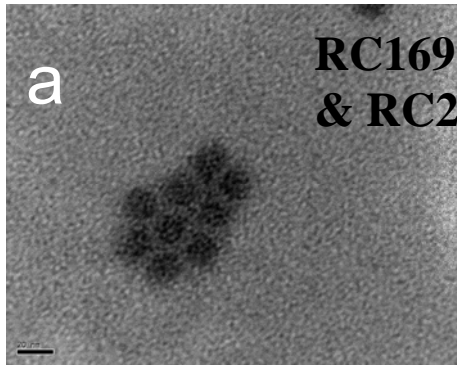


Figure 11: Virus-Like Particles, 300,000x magnification (a) RC169 & RC2 (b) RC2 only (c) R1SG1 & RC2

Figure 12: Dynamic Light Scattering for Particle Size (nm) of Virus-Like Particles (a) RC169 & RC2 (b) RC2 only (c) R1SG1 & RC2

3.6 Encapsidation of the CBDwt-MBP/ISO-s protein by a plant viral nanoparticle

The Hahn group at The University of North Carolina has developed a fluorescent biosensor that can indicate signaling pathways within living cells by imaging protein movements. This technology cannot only identify the movements of proteins within cells, but also look at subtle interactions of protein activities, such as “post-translational modifications, ligand interactions, and conformational changes revealing how the location and subtle timing of protein activity controls cell behavior.” The CBDwt-MBP/ISO-s protein contains a fluorophore and in the presence of a cellular fluorophore, fluorescence resonance energy transfer (FRET) occurs and a unique excitation and emission profile is produced that identifies the presence of endogenous signaling proteins [16,17]. A major drawback of this type of technology is the difficulty in transporting the signaling protein inside the living cell. Encapsidation of this protein by a VLP which has been modified to include a signaling peptide for RME provides an excellent mode of transportation for the molecule of interest.

To achieve the encapsidation, assembly protocols used for the previous VLPs [2] were modified for this application. Initially, the CBD protein will be conjugated to DNA-2 and then incubated with RNA-1 followed by encapsidation with coat protein. 100 μ L 96.4 μ M CBD and 5 μ L 10mg/mL

SMCC was placed in a microcentrifuge and diluted to 1mL with Dulbecco's Phosphate Buffered Saline (DPBS). The tube was vortexed gently and placed on a rocker for approximately 30 minutes at room temperature. After mixing, the contents of the tube was filtered through an Amicon 30,000 MWCO Centricon YM-30 filtration unit (Fisher, U18-007-035) and washed three times with DPBS to remove excess SMCC. The retentate was eluted off of the membrane with three 100 μ L washes of DPBS. 260 μ L of solution containing SMCC linked CBD was recovered. The CBD/SMCC was mixed with 22 μ L of a thiol modified DNA-2 construct and diluted to 1mL. The mixture was vortexed gently and placed on a rocker for approximately 6 hours at room temperature. The contents of the tube were purified as previous using Centricon filtration and stored overnight at 4°C for analysis by Agarose gel electrophoresis. 128 μ L CBD/DNA-2 was mixed with 22 μ L 2.08 μ M RNA-1 transcript and allowed to sit on a rocker for approximately 30min at room temperature. 250 μ L 0.02 μ M Coat Protein was added to tube and brought to 1.0mL volume with DPBS. Entire contents of microcentrifuge tube were removed to a Pierce 0.5-3.0mL 10,000 MWCO Dialysis Cassette (Fisher, PI-66380) and dialyzed against 100mM TRIS Buffer, pH5.5 overnight at room temperature. The contents of the dialysis cassette were removed and purified via sucrose pad. Pelleted PVNs were resuspended by the addition of 200 μ L DPBS and allowing to sit overnight at 4°C. Resuspended PVNs were

evaluated by transmission electron microscopy and dynamic light scattering.

To verify conjugation of the DNA-2 construct to the CBDwt-MBP/ISO-s protein, a 2% agarose gel was run and imaged with visible and ultraviolet light. In Figure 13a, there is a clear indication of protein present in lanes 2,3, 6 and 7. Lanes 6 and 7 contain the protein only, while lanes 2 and 3 show the DNA-conjugated samples. The migration rate of the indicated bands indicates the change in molecular weight due to conjugation of the DNA. The gel was then stained with 1% Ethidium bromide and reimaged under ultraviolet light (Figure 13b). When compared to the DNA-2 only sample in lane 5, it is evident that there is DNA present in lanes 2 and 3, which has migrated at a rate different than expected for DNA alone. Thus, it was determined that the DNA-2 conjugation to the CBD protein was successful.

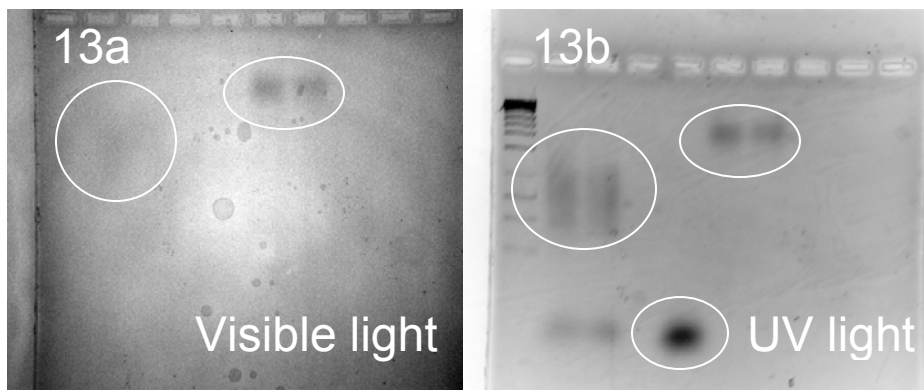


Figure 13: Agarose gel electrophoresis of DNA-2 conjugated CBDwt-MBP/ISO-s Protein. Lane assignments: 1 - DNA ladder, 2,3 – DNA-2/CBD conjugate, 4 – empty, 5 – DNA-2 only, 6,7 – CBD only.

After hybridization of RNA-1 transcript with the DNA-2 conjugated

protein, in vitro assembly of nanoparticles was attempted. As shown in Figure 14, nanoparticle production was indicated by TEM imaging. In Figure 14a, there are a significant number of particles with an indication of icosahedral symmetry, but with somewhat irregular morphology. The trial 2 TEM image (Figure 14b) shows a significantly lower number of particles present, but the same morphological anomaly.

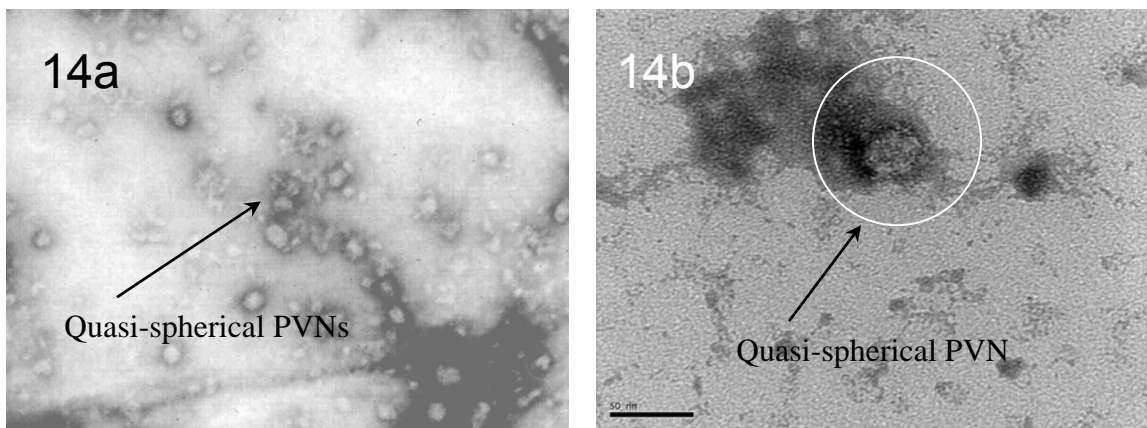


Figure 14: TEM images of CBD PVN – Trial 1. (a) 63,000x magnification (b) 140,000x magnification

Dynamic Light Scattering completed on all samples did not indicate the presence of particles of any size. The limit of detectability for the Malvern zetasizer was determined by serial dilution of native RCNMV particles to be in the femtomolar range. A lack of solubility of the coat protein, with concentrations greater than 1mg/mL, has been a hindrance in the ability to produce an adequate number of nanoparticles for a more complete evaluation.

Chapter 4

***In vivo* testing of RCNMV in Nude mice**

4.1 Introduction

In order to develop RCNMV as a platform for a pharmaceutical vessel, it is necessary to investigate the feasibility of *in vivo* testing for RCNMV. The ability to visualize RCNMV labeled with a fluorophore, FITC, was evaluated at Anticancer Incorporated in San Diego, California. This two-phase study answered the questions of general acute toxicity to animal test models and bioaccumulation in target organs. First, delivery of a significant amount of a fluorescently-labeled RCNMV formulation to Nude mice resulted in no mortality in any of the test subjects and no abnormalities upon gross examination. Second, three weeks post-dose there was no indication of bioaccumulation with examination of the internal organs using an OV100™ whole body fluorescence imaging system. Subdermal delivery of RCNMV produced an obvious signal that reduced in total area over a seven day time period.

4.2 Preliminary assessment of Acute Toxicity and Preliminary Bioaccumulation in Nude mice

The feasibility of *in vivo* testing for RCNMV was evaluated at Anticancer, Incorporated in San Diego, California. This two-phase study answered the questions of general acute toxicity to animal test models and

bioaccumulation in target organs. First, delivery of a significant amount of a fluorescently-labeled RCNMV formulation to Nude mice resulted in no mortality in any of the test subjects and no abnormalities upon gross examination. Second, three weeks post-dose there was no indication of bioaccumulation with examination of the internal organs using an OV100™ whole body fluorescence imaging system. Subdermal delivery of RCNMV produced an obvious signal that reduced in total area over a seven day time period.

4.3 Virus Production

Viral progeny are produced from *in vivo* propagation of the virus in *Nicotiana clevelandii*. This is primarily done by two methods: (1) infecting with transcripts produced *in vitro* from cDNA clones of the viral RNAs inserted into an expression plasmid in which the T7 polymerase promotor and terminator have been cloned [7] and (2) harvesting viruses from plants which have been through several infection cycles..

4.4 Delivery of RCNMV to Nude Mice

Five each Nude mice were given a 40µL intravenous injection of 12mg/mL Red Clover Necrotic Mosaic Virus (RCNMV) labeled with fluorescein isothiocyanate (FITC). External fluorescence scans were done at ½, 1, 2, 3, 4, 6, 12, and 24 hour intervals post dosing. No fluorescence was indicated at any of these time points. In addition, one mouse per week for a

total of three weeks was sacrificed and internal and external scans, Figure 15a and 15b, were completed to provide indication of viral/fluorophore bioaccumulation. Figure 15b shows no indication of internal accumulated fluorescence after week 3.

To verify detectability of fluorescence, one each Nude mouse was given a 50 μ L subdermal injection of 12mg/mL RCNMV labeled with FITC. Fluorescence was checked at 30 minute, 12 hour, 24 hour and 5 day time points. In Figure 15c, the typical yellow/ green color is a clear indication of the presence of fluorescein at the 30 minute time point. The 12 hour time point scan, Figure 15d, shows a marked decrease in the amount of fluorescence. Fluorescence is still present 7 days post-dosing, although significantly reduced from the 12 hour time point scan.

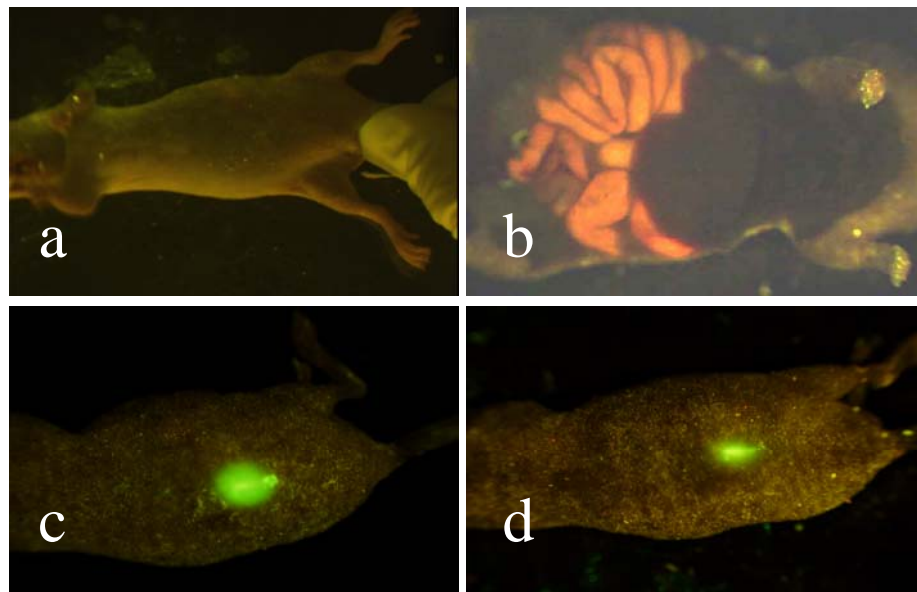


Figure 15: Whole Body fluorescence images of Nude mice.

4.5 Results and Discussion

To summarize, there was no internal or external fluorescence detected. Based on other data, macroscopic detection of fluorescence was not expected due to possible quenching of FITC when exposed to mouse plasma over an extended period of time. An analysis of the intensity of PEG-FITC conjugated to cowpea mosaic virus revealed a rapid quenching within one hour and subsequent loss of signal within four hours [18]. To test this affect, a formulation of RCNMV-FITC was suspended separately in mouse plasma and distilled water. Fluorescence was determined using a Perkin Elmer model LS50B Luminescence Spectrometer. The concentration of each sample was formulated to simulate the *in vivo* study. 20 μ L of 12mg/mL RCNMV-FITC was suspended in 750 μ L of sample (total blood volume for the mouse was estimated at 1.5mL). The pH of the DI water suspension was adjusted to approximately that of the RCNMV-FITC suspension of 7.58. Fluorescence was measured at t=0, 1, 7, and 24 hour time points. As seen in Figure 16, there was a significant drop in the intensity of the RCNMV-FITC sample while there was minimal change in intensity for the DI water sample. Note: Lewis, et. al. showed the PEG-FITC conjugation was microscopically detectable [18].

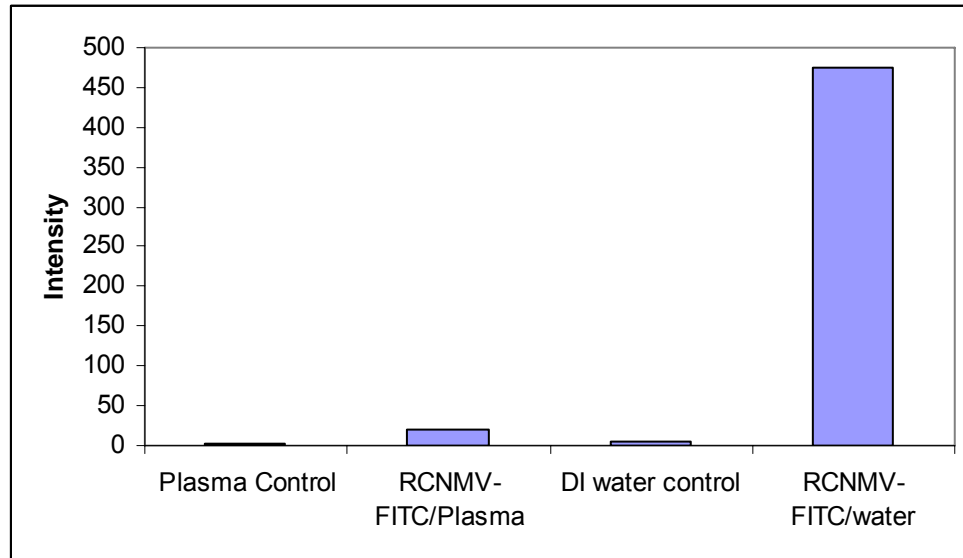


Figure 16: Fluorescence of RCNMV-FITC suspensions at t=1 hour.

The pilot study resulted in no deleterious effects to the mice 3 weeks post-dosing. In addition, there is no detectable bioaccumulation in any internal organs. Finally, the fate of the viral formulation was not determined macroscopically using this method. Therefore, further study is warranted.

Chapter 5

Acute Toxicity, Immunogenicity, Clearance and Preliminary

Biodistribution *in vivo*.

5.1 Introduction

In order to develop PVNs for biomedical applications, it is necessary to understand the activity of RCNMV *in vivo*. While it is generally accepted that plant viruses are not infective when ingested by mammalian organisms [1], the activity of plant viruses or PVNs *in vivo* has not been extensively studied. Here we evaluated the general toxicity of RCNMV by administering a dose that is close to the solubility limit of the virus. Immunogenicity was evaluated by determining the final titer of RCNMV antibodies as determined by ELISA. Clearance and preliminary biodistribution of ¹³¹I –labeled RCNMMV in blood plasma was determination using a Perkin Elmer, WIZARD² Automatic Gamma Counter. These measurements show that PVNs have the attributes needed to function as a delivery vehicle for both drug delivery and fundamental studies of cell biology *in vivo*.

5.2 PVN Dose limit.

Upon arrival, sixteen Balb/c mice (Charles River Labs, Brdigeport, NJ) were allowed to acclimate to the lab for 14 days. Initially, a single animal was dosed intravenously (IV) at a PVN concentration of 2 mg PVN (1.08×10^{13} virus particles) in 70 μ l sterile endotoxin-free PBS. The treated animal was

monitored for 24 hours to determine any adverse effects. With no acute adverse affect, the remaining nine mice were dosed in the following manner. Ten mice received, a dose of 2 mg RCNMV (1.08×10^{13} particles) in 70 μ l sterile endotoxin-free PBS, and 4 control mice received 70 μ l sterile, endotoxin-free PBS by intravenous injection.

5.3 Immunogenicity of PVN.

One day prior to dosage with PVN, a 20ul blood sample was drawn from the lateral saphenous vein from each animal in the study and individual samples pooled by experimental group. On the first day, 10 animals were inoculated with 70ul of 28.6mg/ml PVN and 4 control animals were administered a 70ul buffer solution. A 10-20 ul aliquot of blood will be drawn at days 0, 1, 3, 5, 7 and 14 and 21 post-inoculation from the lateral saphenous vein. To assess any secondary immune response, 6 of the mice were administered a booster dose of PVN intravenously at the initial concentration after the one week time point. At the completion of the study, the final titer of the PVN antibodies was determined by ELISA.

5.4 Radiolabeling of PVN

The plant virus nanoparticles were labeled with ^{131}I using Iodo-Gen Pre-coated iodination tubes (Thermo Scientific) following manufacturers protocol. Sodium iodide was purchased from Perkin Elmer (Shelton, CT) with a specific activity of 185GBq/mg. Enough PVN to deliver 100ug to each animal was

labeled. Separation of the unbound ^{131}I from the labeled RCNMV was performed using a NAP -10 (GE Healthcare) desalting column. Concentration of the PVN post-labeling was determined using a Coomassie Plus Protein Assay Reagent (Pierce Scientific).

5.5 Clearance rate determination and preliminary biodistribution

^{131}I radio-labeled PVN was administered to the animals, by intravenous (IV) injection, at the dosage determined in PVN dose limit experiment. The PVN was formulated such that each animal would receive no more than 5 uCi of radiation. Aliquots of 10-20ul of blood was drawn from a lateral saphenous vein bleed at 9 time points (pre injection, 15 and 30 minutes, 1, 2, 4, 8, and 24 hours and day 2 and 3) to determine the level of PVN circulating in the blood stream.

The cumulative amount of blood drawn from each animal was recorded with a total of no more than 200ul or 1% of their body mass drawn over the course of the study. Ten mice were administered ^{131}I -labeled PVN, two control mice were administered ^{131}I and 4 control animals were administered a buffer control. The circulating half-life was determined based on detectable radioactivity in serum collected from the animal. Three days after the initiation of the clearance study, all animals were euthanized by administration of a lethal dose of xylazine (2 mg/mL)/ketamine (16 mg/mL) followed by a cervical displacement. A necropsy was performed on each animal and major

organs harvested to determine the level of PVN accumulation based on levels of ¹³¹I radioactivity retention in the individual organs. The major organs that were harvested include brain, lungs, heart, thymus, spleen, kidney, thyroid, liver, stomach, upper gastrointestinal tract, lower gastrointestinal tract, skin and bone. The harvested organs were placed in scintillation vials, masses taken, and radioactivity counts determined using a Perkin Elmer WIZARD² Automatic Gamma Counter.

5.6 Results and Discussion.

Acute toxicity was determined near the solubility limit of RCNMV and well above the expected dose of a final formulation. 2mg of RCNMV (70uL 28.6mg/mL) was delivered by intravenous (IV) injection via the tail vein of a Charles River Labs, Inc. Balb/c mouse. The mouse was monitored over the next 24 hours for any deleterious effects. 24 hours post-inoculation the mouse had survived and was exhibiting normal behavior: grooming, nesting, etc. Seven additional mice received injections (6 IV, 1 SubQ). In addition, 4 mice were dosed with Phosphate Buffered Saline (PBS) as a control group. The mice were observed for 21 days for any sign of aberrant behavior. Post-mortem intracardiac bleeds were done on each group and pooled for preliminary determination of immunogenicity. After evaluation by ELISA, no discernible levels of antibody above background were indicated and the study

commenced to Phase II.

Immunogenicity was determined by dosing the animals with 70ul RCNMV (28.6mg/ml). Prior to dosage with PVN, a ~20ul blood sample was drawn from the lateral saphenous vein of each mouse animal on study and individual samples pooled by experimental group. On day 1, 10 animals were inoculated with PVN and 4 control animals were administered PBS. A 10-20ul aliquot of blood was drawn at days 0, 1, 3, 5, 7 and 14 and 21 post-inoculation from the lateral saphenous vein of each animal and pooled. To assess any secondary immune response, 6 mice were administered a boost dose of PVN at the initial concentration after the one week time point. At the completion of the study, the final titer of the PVN antibodies was determined by ELISA. In Table 1, there was no significant amount of absorbance when compared to a control with a primary rabbit antibody known to bind the RCNMV coat protein. The pooled mouse plasma of the dosed groups showed no significant amount of absorbance above that of the PBS control group.

Table 1. UV-VIS absorbance of pooled mouse plasma samples as determined by ELISA.

Sample	Absorbance
RCNMV/Rabbit	2.59275
t=0, Control	0.001125
t=0, Dosed	0.0035
t=1, Control	0.026125
t=1, Dosed	0.021375
t=3, Control	0.04425
t=3, Dosed	0.03125
t=5, Control	0.043875
t=5, Dosed	0.029375
t=7, Control	0.009
t=7, Dosed	0.05125
t=0, Boosted Dose	0.054
t=14, Control	0.012125
t=14, Dosed	0.005875
t=7, Boosted Dose	0.01475
t=21, Control	0.027625
t=21, Dosed	0.018125
t=21, Boosted Dose	0.0455

To determine the clearance rate of circulating RCNMV *in vivo*, Balb/c mice were administered the virus iodinated with ¹³¹I. Aliquots of 10-20ul of blood were drawn from a lateral saphenous vein at 9 time points (pre injection, 5 (5 mice), 15 and 30 minutes and 1, 2, 3, 24, and 48 hours) to determine the level of RCNMV circulating in the blood stream. Ten mice were administered ¹³¹I-labeled RCNMV, 2 mice (test subjects 2 and 10) were given ¹³¹I and 1 control animal (test subject 4) was dosed with PBS. Test subject 2 was given a larger dose of ¹³¹I. The circulating half-life was determined based on detectable radioactivity in serum collected and averaged over all test

subjects. In figure 17, it was determined that the circulating half-life for RCNMV is less than 15 minutes. There was an increase in radioactivity detected in the blood samples over

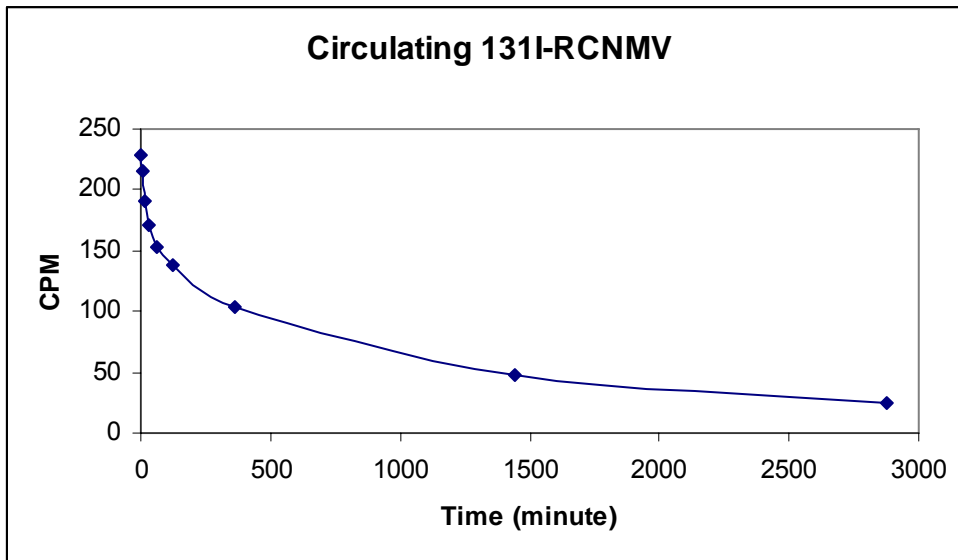


Figure 17: Circulating ^{131}I -labeled RCNMV as determined by detectable radioactivity in mouse plasma.

the first few minutes post-inoculation. Additionally, 90% of the radioactivity had been eliminated within 24 hours.

To provide preliminary data in preparation of a larger bio-distribution study, the test subjects were euthanized by a lethal dose of Xylazine/Ketamine. Secondary methods of euthanasia were cervical dislocation and thoracotomy. A necropsy was performed and major organs harvested to determine the level of iodinated RCNMV accumulation based on

levels of ^{131}I radioactivity within target organs. The major organs harvested include heart, lungs, spleen, liver, kidney, stomach, small intestine, large intestine, skin, muscle, bone, brain, bladder, thyroic, and tail. The harvested organs were placed in scintillation vials and evaluated for residual radioactivity. The counts are reported in Table 1. Animals 2 and 10 were dosed with ^{131}I only as positive controls. Animal 4 was dosed with Phosphate Buffered Saline as a negative control. Animals 2 and 3 were given a 200uL dose on day 0 post-iodination of RCNMV. Animals 4-9 were dosed on day 1 post-iodination of RCNMV. Animals 10-15 were dosed day 2 post-iodination of RCNMV. There was no statistically significant accumulation in the indicated internal organs across the dose groups. As expected, there was significant accumulation in the thyroid for the ^{131}I control group. Animals 2 and 3 were given higher than normal dose volume. Therefore, it can be inferred the volume of material was more than tolerable by the IV injection method used. Some of the test material may have diffused into surrounding tissues and normal grooming activities could have resulted in higher than expected counts in the gastrointestinal tract of the animals.

The total amount of activity of test material was calculated by extrapolation from a best fit curve of the circulating activity of the ^{131}I -RCNMV formulation post-inoculation. The percentage of material remaining was calculated based on the total amount of activity and the average counts from each dose group.

Only animal number 10 of the positive control group was counted. 48 hours post-inoculation there was less than 3% activity in the test group and less than 6% activity in the positive control group. There is a 0.11% retention of activity in the thyroid of the test group and 0.93% in the positive control. The elevated count for the control group is expected due to the tendency of free ¹³¹I to accumulate in the thyroid [8,9,10]. Additionally, there was significant activity remaining in the tail: 0.81% for the test group and 1.96% for the positive control. This could be the result of test material delivered to the tissues surrounding the site of injection. Higher than average counts for the stomach, upper gastrointestinal tract and lower gastrointestinal tract of the control animal provides another indication of some extraneous test material at the site of injection. All calculations are based on a total dose applied to each animal of 220,000 counts as a baseline of the test material taken at time of dosing. To estimate the applied dose, a best fit curve was applied to the graph for circulating half-life, figure 18. The trendline was extrapolated to the y-axis and the area under the curve was calculated as the average total number of counts delivered to the animals.

As available, random urine samples were collected throughout phase III. As seen in Table 2, high levels of radioactivity were present in all samples at earlier time

Table 2. Average counts of random urine samples at varied time points.

Time (Min)	DPM
15	1150
60	2500
120	3450
360	3550
1080	275
2280	6

points from animals dosed with radiolabeled RCNMV. Assuming the average urine output for a mouse is 1-2MI [11,12] and considering the total number of counts for the 5 time points at 10uL per time point results in an estimated evacuation of 218,500-437000 counts which corresponds to the estimated delivered dose. This indicates nearly all the virus may have been evacuated through the urine.

Chapter 6

In Vitro Luminescence of Luciferin-infused RCNMV Conjugated with Adenoviral Derived Targeting Peptides.

6.1 Introduction

Having established that RCNMV has potential for *in vivo* diagnostic applications, we turn our attention to the capabilities of a PVN formulation. As an initial step, RCNMV was infused with luciferin and then conjugated to a targeting peptide shown to have activity in HeLa cells[33]. These formulations were dosed to a HeLa variant line, HeLa-Luc® (Xenogen, HeLa-luc(P9) cervical), which is engineered to express luciferase. In the presence of luciferin, the cells will luminesce. A change in the activity of Luciferin, free versus packaged, should be seen.. Additionally, a new method for imaging the virus *in vivo* is being investigated by the research group of Dr. Gregg Dean at North Carolina State Universities Veterinary School. This technology would be dosed to luciferase expressing mice and whole body imaging completed to visualize biodistribution of the PVN and verify data presented in Chapter 5 of this thesis.

6.2 Infusion of Luciferin into RCNMV [5]

An aliquot of RNCMV was received and purified by passing through a illustra® NAP-10® column (GE, part number 17-0854-01 Sephadex® G-25 DNA Grade column). 500uL fractions were collected. Concentrations were determined using a Nanodrop® UV/VIS spectrophotometer. 5mg RCNMV

was diluted to 1mL with 200mM NaOAc buffer, pH 5.2. 100uL 2M Tris buffer, pH 8.5 and 20uL 1M EDTA, pH 8 was added to tube and allowed to incubate at rt for ~30 minutes. 50uL 86.2mM Luciferin (Sigma-Aldrich, part number L6882) was added. The tube was covered with foil and rocked overnight at room temperature. After incubation, 125uL 100mM NaOAc, 50mM CaCl₂, 50mM MgCl₂, pH 5.5, was added to the tube and incubated at rt for ~30 minutes. The tube was centrifuged at 10,000rpm for 5 minutes and supernatant collected. The Luciferin-infused RCNMV was loaded onto a NAP-25® column (GE, part number 17-0852-01 Sephadex® G-25 DNA Grade column). ~250uL fractions were collected and most concentrated aliquots were pooled. A 100uL sample was set aside to use as a control.

6.3 Conjugation of Targeting Peptides [32,33]

2-3mg Sulfo-SMCC (Thermo Scientific, part number 22322, lot# JE122737A) in 50uL DMSO was added to a 500uL aliquot of Luciferin-infused RCNMV and incubated at room temperature for ~30 minutes. Free Sulfo-SMCC was removed by passing through a NAP-25® column equilibrated with 20mM HEPES, pH 7.2. Fractions were collected and analyzed with Nanodrop UV/VIS spectrophotometer. Concentrations of fractions were determined and the most concentrated were combined and used for two different targeting peptide conjugations. 2 mg. of each peptide in 50uL DMSO was added to the SMCC bound RCNMV and rocked overnight at room

temperature. Two different targeting peptides were used. The first is a CD46 Adeno-derived nuclear localization signal (NLS) (CGGSTSLRARKA-TAMRA) which includes the fluorophore TAMRA (used to verify binding of peptide via UV/VIS). The second is an Adeno-derived receptor mediated endocytosis (RME) signal (CGGKKKKKKKSEDEYPYVPNFSTSLRARKA). Excess peptide was separated using a G100 column equilibrated with HEPES, pH7.2 500uL fractions were collected and concentration of RCNMV and peptide were determined using UV/VIS spectroscopy and Luciferin concentration by fluorescence.

6.4 Preparation of samples and delivery to HeLa luciferase expressing cells

With the formulated samples and appropriate controls in hand, two-fold dilutions were done on each sample in preparation for delivery to previously prepared plates containing HeLa-luc cells. 100uL of each sample during the formulation process was reserved for delivery to cell plates. A serial dilution was performed on 9 samples, according to Table 3.

Table 3. Sample identification for delivery to HeLa-luc cell plates.

Sample Name	Sample i.d.	Location
Luciferin-infused CD46-TAMRA conjugated RCNMV	^{CD46} RCNMV ^{Luc}	Plate 1, 1-3
Luciferin-infused RME conjugated RCNMV	^{RME} RCNMV ^{Luc}	Plate 1, 4-6
Luciferin-infused RCNMV	RCNMV ^{Luc}	Plate 1, 7-9
Luciferin-infused SMCC linked RCNMV	^{SMCC} RCNMV ^{Luc}	Plate 2, 1-3
SMCC linked RCNMV	^{SMCC} RCNMV	Plate 2, 4-6
Red Clover Necrotic Mosaic Virus	RCNMV	Plate 2, 7-9
CD46 Adeno-derived nuclear localization signal (NLS) (CGGSTSLRARKA-TAMRA)	CD46	Plate 3, 1-3
Adeno-derived receptor mediated endocytosis (RME) signal (CGGKKKKKKKSEDEYPYVPNFSTSLRARKA)	RME	Plate 3, 4-6
Buffer	Buffer	Plate 3, 7-9
Luciferin	Luc	Plate 1-3, 10-

100uL of each sample was placed in row B of a sterile 96-well plate. 100uL of EMEM media (10%FBS) were added to rows C-G for each sample to be tested. 100uL of media was added to each sample in row B. 100uL of dilution in row B was removed and added to Row C. 100uL of dilution in row C was removed and add to Row D. This process was repeated for rows D through G. Media was removed from 3 HeLa-Luc® (Xenogen, HeLa-luc(P9 cervical) luciferase expressing cell plates incubated for 48 hours. 100uL of concentrated samples retained during sample preparation were added to row A of cell plates. Samples from each well of the dilution plate were transferred to corresponding wells on cell plates. Columns 10-12 of the cell plates were inoculated with Luciferin as a positive control to compare performance of cell plates. Plates were read for luminescent intensity (545nm/40, S=250) at 0,

15, 30, 45, 60, 75, 90, 105, 120 minutes and at 4, 6, 8, 12 hours on a BioTek Synergy HT® plate reader.

6.5 Results and Discussion

Red clover necrotic mosaic virus (RCNMV) was infused with luciferin. The concentration of virus present in the sample was determined by UV/VIS absorbance @ 260nm ($\epsilon=38480 \text{ M}^{-1}\text{cm}^{-1}$). The concentration of luciferin was determined by fluorescent intensity (545 nm, S=250) compared to a standard curve, Figure 18. The ratio of Luciferin to RCNMV for all samples

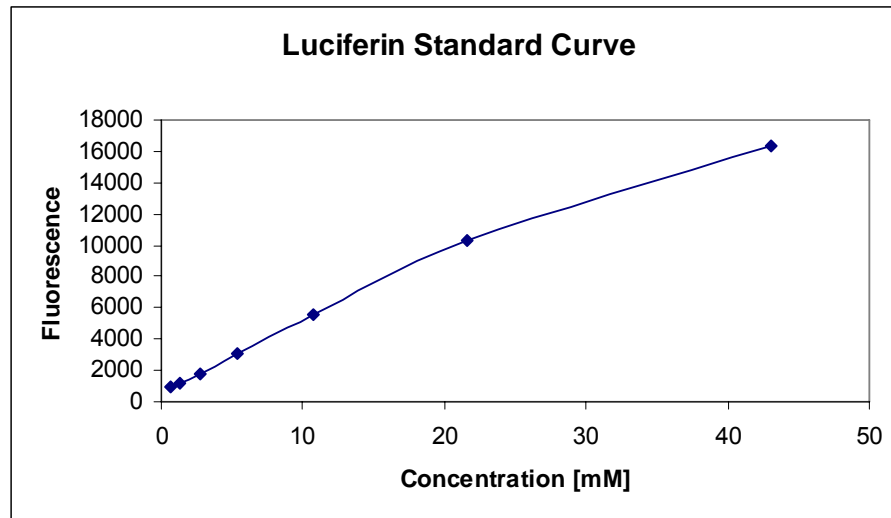


Figure 18: Standard curve of luciferin concentration dosed to HeLa-luc cells.

for all samples was found to be between 180-240:1. Two different peptides previously shown to target HeLa cells[32,33] were conjugated to the virus and delivered to HeLa-luc cells to determine if targeted PVNs infused

with a cargo would increase efficacy. 3 plates of HeLa-luc cells with an appropriate number of time points were used with appropriate controls outlined in the experimental section. Background luminescence as determined in the negative control was negligible. Positive controls of free luciferin were included on each plate to ensure activity of the cells and provide a standardization to compare each plate, Figure 20. All luciferin controls exhibited a maximum luminescence at the 30 minute time point with comparable results for all 3 plates.

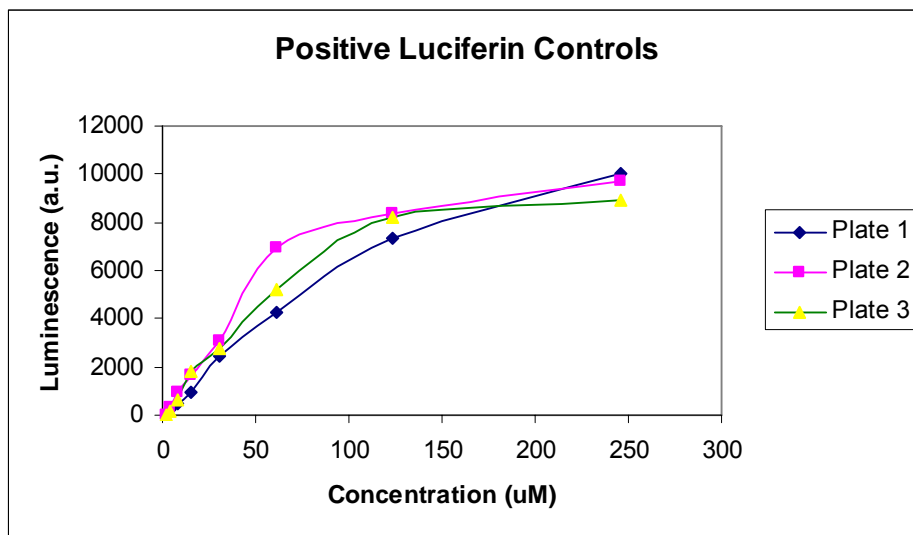


Figure 19: Luciferin only controls at the 30minute time point for HeLa-luc plates 1, 2, and 3.

Luminescence was evident over a 1.5 hour time period. All other controls and formulated samples showed no luminescence over background at any time point. There are several possible scenarios for failure of this assay. For example, the targeted formulation may be taken up by the cells, but

subsequently the cargo may not be released. The specific targeting peptides may not be able to target the HeLa-luc cell line.

Chapter 7

Conclusion

Red clover necrotic mosaic virus is an excellent building block as a tool to advance the treatment of disease. The structure of the virus allows for its use as a carrier for small molecules that can be targeted to specific cells. As an initial step, it was desired to explore the possibility of alternative ways to produce the virus which would decrease the propagation time in a more controlled environment. It was possible to assemble the virus *in vitro* using transcript RNAs and capsid protein harvested from disassembled wild type virus. While the assembly process itself was efficient, the amount of RCNMV produced is limited by the solubility of the capsid protein. However, It is possible to assemble particles of varying RNA composition and encapsidate novel substances [2]. Using current technology to propagate virus, the effect in mammalian systems must be evaluated. While it is accepted that plant viruses do not infect animal hosts, it is necessary to understand any effects when giving the virus by unusual routes of administration. I discovered that intravenous injection of native virus into mice gave no deleterious effects. The mice suffered no acute toxicity, no detected immune response and no evidence of biodistribution in any of the internal organs. Thus, I carried out the formulation of a PVN using native RCNMV designed to visualize the ability of the virus to enter cells and verify biodistribution *in vivo*. To verify

uptake the virus by cells, I infused native RCNMV with luciferin and attached targeting peptides. The peptides had previously been shown to target HeLa cells. I used a HeLa strain that overexpresses luciferase. When the luciferin comes in contact with luciferin, it reacts and luminesces. While, it was possible to see the reaction of free luciferin, there was no indicated change using the PVN as a carrier. So, either the PVN didn't localize to the cytoplasm, or if it did, the cargo wasn't released. This warrants further investigation to verify the cells actually internalize the PVN and optimization of targeting moieties.

References

1. Temple University (1998, May 18). Study Highlights The Use Of Viruses As Tools For Material Science And Drug Delivery. *ScienceDaily*. Retrieved November 29, 2007, from <http://www.sciencedaily.com/releases/1998/05/980518061624.htm>
2. Loo, L., et al., *Controlled encapsidation of gold nanoparticles by a viral protein shell*. *Journal of the American Chemical Society*, 2006. 128(14): p. 4502-4503.
3. Douglas, T. and M. Young, *Host-guest encapsulation of materials by assembled virus protein cages*. *Nature*, 1998. 393(6681): p. 152-155.
4. Lommel, S.A., *Targeted Delivery with a Plant Viral Nanoparticle.*, N.S.U.D.o. Toxicology, Editor. 2006: Raleigh.
5. Loo, L., et. al, *Infusion of Dye Molecules into Red Clover Necrotic Mosaic Virus*, *Chemical Communications*, 2008, DOI: 10.1039/b714748a
6. Basnayake, V.R., Sit, T.L., and Lommel, S.A., *The genomic RNA packaging scheme of Red clover necrotic mosaic virus*, *Virology*, 2006, 345: p. 532-539.
7. Kim, K.H. and S.A. Lommel, *Sequence element required for efficient -1 ribosomal frameshifting in red clover necrotic mosaic dianthovirus*. *Virology*, 1998. 250(1): p. 50-59.
8. Sherman, M.B., et al., *Removal of divalent cations induces structural transitions in Red clover necrotic mosaic virus, revealing a potential mechanism for RNA release*. *Journal of Virology*, 2006. 80(21): p. 10395-10406.
9. Gillitzer, E., et al., *Chemical modification of a viral cage for multivalent presentation*. *Chemical Communications*, 2002(20): p. 2390-2391.
10. Callaway, A., et al., *The multifunctional capsid proteins of plant RNA viruses*. *Annual Review of Phytopathology*, 2001. 39: p. 419-+.
11. Xiong, Z. and Lommel, S., *Red Clover Necrotic Mosaic Virus Infectious Transcripts Synthesized In Vitro*, *Virology*, 1991, 182: p. 388-392.

12. Zhao, X, Fox, J., et. al., In vitro assembly of Cowpea Chlorotic Mottle Virus from Coat Protein Expressed in Escherichia coli and In Vitro-Transcribed Viral cDNA, *Virology*, 1995, 207: p. 486-494.
13. Phelps, J., et. al., Expression and self-assembly of cowpea chlorotic mottle virus-like particles in *Pseudomonas fluorescens*., *Journal of Biotechnology*, 2007, 128: p. 290-296.
14. Fox, J., et. al., Comparison of the Native CCMV Virion with In Vitro Assembled CCMV Virions by Cryoelectron Microscopy and Image Reconstruction., *Virology*, 1998, 244: p. 212-218.
16. Hahn, K., Touthkine, A., Live-Cell fluorescent biosensors for activated signaling proteins, *Current Opinion in Cell Biology*, 2002, 14: p. 167-172.
17. Nalbant, P, et. al., Activation of Endogenous Cdc42 Visualized in Living Cells, *Science*, 2004, 305: p. 1615-1619.
18. Lewis, J., et. al, Viral nanoparticles as tools for intravital vascular imaging, *Nature Medicine*, 2006, 12: p. 354-360.
19. *How Do You Make A Transgenic Plant?*, 2004, <<http://cls.casa.colostate.edu/TransgenicCrops/how.html>>, date accessed: 05/04/2007.
20. Temple University (1998, May 18). Study Highlights The Use Of Viruses As Tools For Material Science And Drug Delivery. *ScienceDaily*. Retrieved November 29, 2007, from <http://www.sciencedaily.com/releases/1998/05/980518061624.htm>
21. Loo, L., et al., *Controlled encapsidation of gold nanoparticles by a viral protein shell*. *Journal of the American Chemical Society*, 2006. 128(14): p. 4502-4503.
22. Douglas, T. and M. Young, *Host-guest encapsulation of materials by assembled virus protein cages*. *Nature*, 1998. 393(6681): p. 152-155.
23. Lommel, S.A., *Targeted Delivery with a Plant Viral Nanoparticle.*, N.S.U.D.o. Toxicology, Editor. 2006: Raleigh.
24. Loo, L., et. al, Infusion of Dye Molecules into Red Clover Necrotic Mosaic Virus, *Chemical Communications*, 2008, DOI: 10.1039/b714748a.

25. sherman, M.B., et al., Removal of divalent cations induces structural transitions in Red clover necrotic mosaic virus, revealing a potential mechanism for RNA release. *Journal of Virology*, 2006. 80(21): p. 10395-10406.
26. Xiong, Z. and Lommel, S., Red Clover Necrotic Mosaic Virus Infectious Transcripts Synthesized In Vitro, *Virology*, 1991, 182: p. 388-392.
27. Rockall, TA, Watkinson, JC, Clark, SE, Douek, EE, *Scintigraphic evaluation of glomus tumours*. *J Laryngol Otol*. 1990 Jan;104(1):33-6.
28. Molotkov, OV, Kozlov, NB, *Thyroid gland function in heatstroke*. *Biull Eksp Biol Med*. 1975 Jul;80(7):21-4. Russian.
29. D'Angelo, SA, *I131 and P32 accumulation in anuran thyroid gland in normal and accelerated metamorphosis*. *Proc Soc Exp Biol Med*. 1956 Aug-Sep;92(4):693-8.
30. Birder, LA, et.al., *Altered urinary bladder function in mice lacking the vanilloid receptor TRPV1*, *Nature Neuroscience*, 5, 2002, 856 – 860, Published online: 5 August 2002, Accessed 08/14/08.
31. Wood R, Eichel L, Messing E, Schwarz E, Automated Noninvasive Measurement of Cyclophosphamide-induced Changes in Murine Voiding Frequency and Volume. *The Journal of Urology* , Volume 165 , Issue 2 , 653 – 659.
32. Zhang, et.al., *A transfecting peptide derived from adenovirus fiber protein*, *Gene Therapy*, 1999, 6,, p. 171-181.
33. Tkachenko, et.al., *Multifunctional Gold Nanoparticle–Peptide Complexes for Nuclear Targeting*, *J. Am. Chem. Soc.*, 2003, 125 (16), pp 4700–4701